

Investigation of Void Linkage in Magnesium Using SEM and Micro Computed X-ray Tomography

Michael J. Nemcko^{1,*}, David S. Wilkinson¹

¹ Department of Materials Science and Engineering, McMaster University, Hamilton L8S 4L8, Canada

* Corresponding author: nemckomj@mcmaster.ca

Abstract Ductile fracture in metallic materials occurs by the nucleation, growth, and linkage of microvoids within the bulk of the material. As a result, two dimensional techniques must be complimented with three dimensional techniques in order to completely characterize the fracture process. In the present study, tensile testing coupled with: scanning electron microscope (SEM) imaging, electron backscattered diffraction (EBSD) patterning, and micro computed x-ray tomography (XCT), have been used to analyze void linkage in magnesium, which exhibits poor formability at room temperature. SEM imaging and EBSD patterning have been used to characterize the mechanisms responsible for void linkage and to determine the effects of void fraction and void orientation on the failure strain. Micro XCT has been used to examine the evolution of internal voids. It has been established that void fraction and void orientation have a weak influence on the failure strain due to the premature linkage of voids. EBSD analysis has shown that this premature void linkage is associated with the failure of twin and grain boundaries. The results suggest that (in contrast with more ductile fcc metals) the local microstructure has a significant impact on void linkage.

Keywords Magnesium, Void Linkage, Micro computed tomography

1. Introduction

Magnesium exhibits limited ductility when deformed at room temperature. The HCP crystal structure of the material does not provide an adequate amount of slip systems to satisfy the von Mises criterion. As a result, mechanical twins are activated to accommodate stress concentrations [1]. Void nucleation typically occurs within the bulk of the material. As a result, characterization techniques which can detect internal flaws are required to fully understand fracture. In the past, model materials were fabricated to better understand void growth and coalescence [2]. The 2D model materials consisted of thin sheets containing laser drilled holes through the thickness which simulated voids [3]. These model materials were pulled in tension within the SEM such that the growth and linkage of the holes could be analyzed in increments of deformation. FCC materials (aluminum and copper) were studied which are more isotropic than HCP materials. The results showed that void growth was uniform. Linkage of the voids occurred by the internal necking mechanism observed by Puttick [4]. Furthermore, experiments were carried out to determine the effects of the void fraction and void orientation on the failure strain. It was concluded that both parameters had a strong correlation with the failure strain.

The experiments were then extended to 3D to determine if the 2D experiments were representative of what occurs in the bulk [5]. 3D model materials were fabricated by diffusion bonding multiple sheets containing laser drilled holes between hole free sheets. These were used to simulate a 3D distribution of internal voids. The 3D model materials were tested in situ. The voids in the material are resolved using x-ray tomography from a synchrotron source based on the difference in the attenuation coefficient between the metal and the void. The use of tomography in materials science has significantly increased in the past few years [6]. In the present work, tomography is coupled with EBSD and SEM to understand the fracture of magnesium materials which display mechanical anisotropy.

2. Experiments

Commercially pure magnesium was hot rolled to a thickness of 125 μm . Tensile specimens were machined using electrical-discharge wire cutting. The tensile specimens had a reduced gage section with a length of 2 mm and a width of 1 mm. The samples were polished with 0.05 μm colloidal silica to ensure a smooth surface for laser machining. Holes with a diameter of approximately 13 μm , were laser drilled into the gage section of the tensile samples using a Ti:sapphire laser system. For one set of experiments, samples with a single row of holes perpendicular to the tensile axis were tested with different center to center hole distances to examine the effects of void fraction on the failure strain. The distances used were 40, 55 and 70 μm . In another set of experiments, samples with a single row of holes oriented at various angles with respect to the tensile direction were tested to analyze the effects of void orientation on failure strain. The angles were 45, 60 and 75°. After laser drilling, the samples were annealed in a tube furnace purged with argon, at 450 °C for 1 hour, to remove the heat affected zone in the vicinity of the holes. The average grain size was approximately 50 μm with a standard deviation of 25 μm , after the final annealing process.

EBSD patterns were obtained to determine the initial texture in the vicinity of the holes. Tensile tests coupled with electron microscopy have been used to visualize void growth and linkage in-situ. Samples were pulled in uniaxial tension at room temperature under the SEM. The tensile stage utilizes a 220 N load cell and experiments were carried out at a constant test speed of 10 $\mu\text{m/s}$. Images were obtained in increments during deformation. Tests were stopped when microstructural features or damage was observed. EBSD was carried out on the deformed samples and micro computed tomography scans were employed to observe the bulk of the deformed samples. The Skyscan 1172 micro computed tomography unit was used in the analysis.

3. Results

The EBSD patterns obtained on the deformed samples allowed for characterization of the microstructural features which led to failure. Figure 1 shows the SEM image series of a row of holes perpendicular to the tensile axis with a center to center hole distance of 40 μm . The EBSD patterns have been overlaid on the SEM images where necessary.

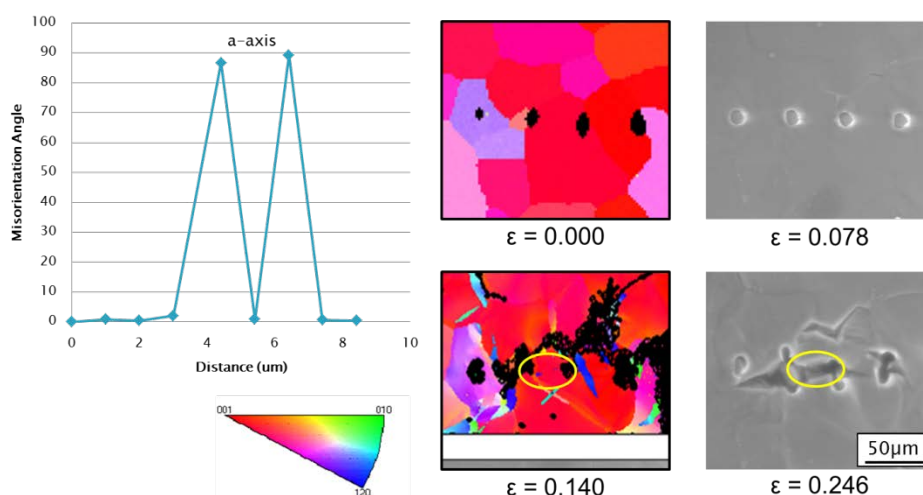


Figure 1: SEM image series at various far field strains and misorientation profile across the twin circled.

At a far field strain of 0.14, a twin was resolved which is circled in Figure 1. The twin was identified as an extension twin, which forms along the $\{10\bar{1}2\}$ plane in magnesium. The misorientation profile in Figure 1 displays a rotation of approximately 86° about the $\langle 11\bar{2}0 \rangle$ direction (a-axis) with respect to the parent grain. This geometrical relationship is characteristic of the extension twin. The twin became a site for crack propagation at a far field strain of 0.246. It has been established that extension twins form at lower stresses to accommodate extension along the $\langle 0001 \rangle$ direction (c-axis). However, once nucleated the twins become stress concentrators and eventually become failure sites.

Figure 2 shows the SEM image series of a row of holes perpendicular to the tensile axis with a center to center hole distance of $70\ \mu\text{m}$. EBSD patterns were overlaid in the increments where they were obtained.

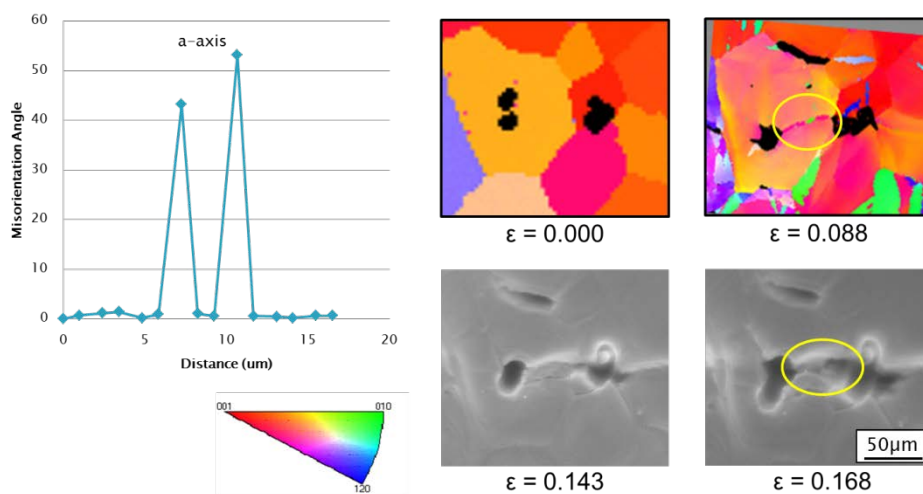


Figure 2: SEM image series at various far field strains and misorientation profile across the twin circled.

A twin was resolved by EBSD at a far field strain of 0.088 which is circled in Figure 2. The twin was characterized as a compression twin, which forms along the $\{10\bar{1}1\}$ plane in magnesium. The misorientation profile in Figure 2 reveals a rotation which is approximately 56° about the a-axis with respect to the parent grain. This is characteristic of the compression twin which accommodates compression along the c-axis. The twin boundary failed at a far field strain of 0.168. It has been established that this twin type requires high stresses to activate. The twin nucleated at a relatively low far field strain. This suggests that a complex stress state occurs within the material. Some grains experience much higher stresses than others due to the mechanical anisotropy of the material. Figures 1 and 2 both show failure at grain boundaries. Grain boundary failure is another dominant fracture mechanism.

The effects of void fraction on failure were observed by performing tests on void rows with different center to center holes distances. The center to center hole distance can be related to the void fraction f by

$$f = \frac{2r}{\lambda} \quad (1)$$

where r is the radius of the hole and λ is the center to center spacing. The normalized length of the

voids which contributed to the first crack was plotted as a function of the void fraction. The normalized length in the tensile direction represents the local displacement field within the vicinity of a void. The results are shown in Figure 3.

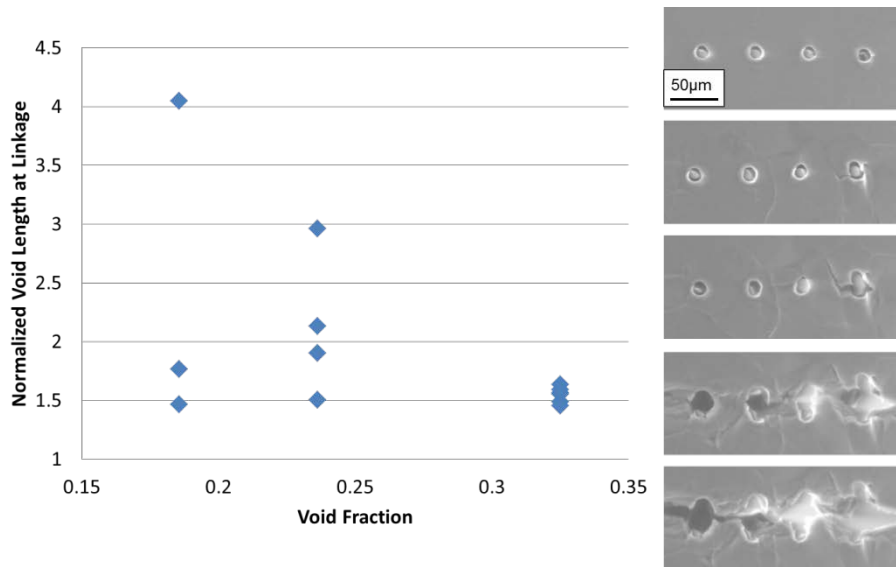


Figure 3: Normalized void length vs. void fraction.

The data does not show a strong correlation between the void lengths at failure and void fraction. This is different from what has been observed in isotropic materials. The variability of the data for a given void fraction suggests that the voids do not grow uniformly.

The effects of void orientation on failure were examined by testing samples with the holes oriented at various angles from the tensile axis. The center to center spacing of the holes was held constant in these experiments at 40 µm. The results are shown in Figure 4.

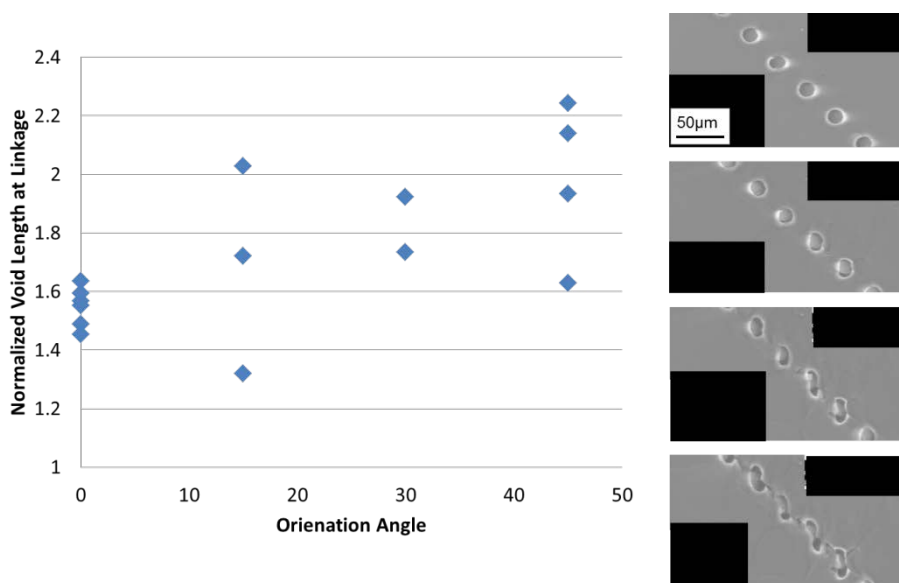


Figure 4: Normalized void length vs. void orientation.

The correlation between the void lengths at failure and void orientation is not strong. This is different from what was predicted in the work of Hosokawa et al [5]. However, in the previous work isotropic materials were tested where void growth was uniform and linkage occurred by internal necking of the voids. In the magnesium materials tested premature linkage occurs by grain and twin boundary failure. Therefore, the weak relationship between the void fraction and void orientation can be attributed to the fact that the linkage of the holes is not driven solely by plasticity in the magnesium materials tested.

Micro XCT has been used to investigate the bulk of the deformed samples. Figure 5 shows a deformed sample with a row of voids perpendicular to the tensile axis with a center to center hole distance of 70 μm . A grain boundary crack was detected by SEM shown in Figure 5a). The reconstructed 3D volume is shown in Figure 5b).

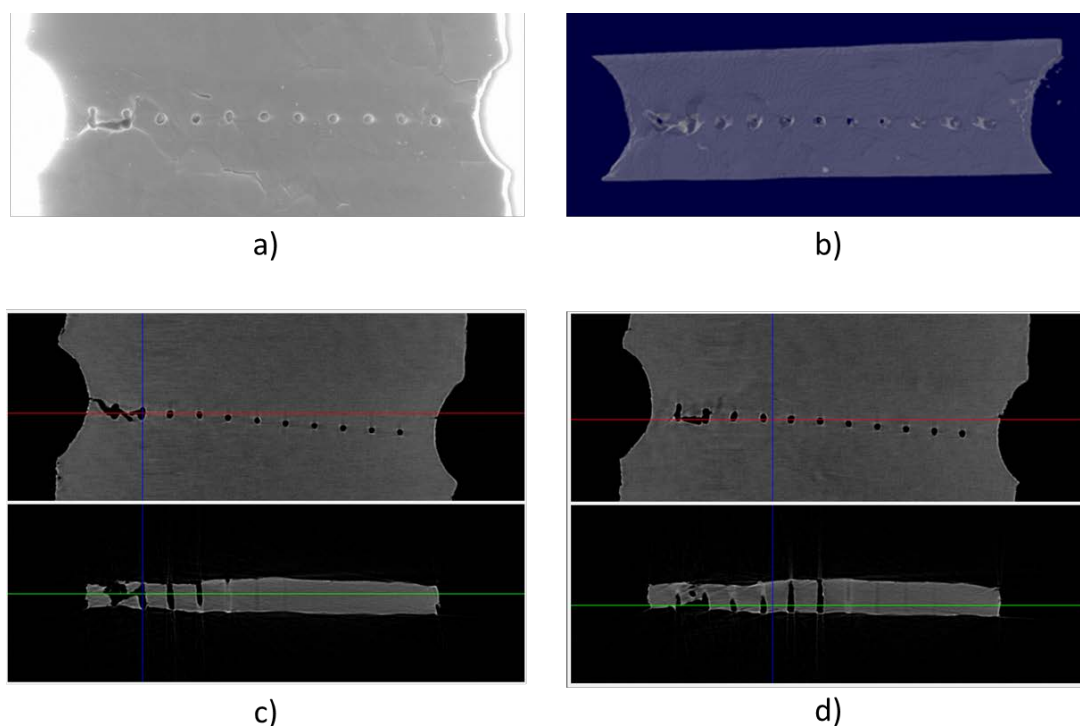


Figure 5: a) SEM image b) Reconstructed 3D volume c) Data slice at the back of the sample d) Data slice at the front of the sample.

The volume was examined using the Data Viewer software developed by SkyScan which allows the user to view the reconstruction slice by slice. Figure 5c) reveals that a crack has already developed on the side of the sample which cannot be detected by SEM. Figure 5d) shows the depth of the crack that is shown in the SEM image. The results suggest that the failure of the materials tested is very complex and the 3D structure must be accounted for to accurately predict the failure of these materials.

4. Discussion

Void linkage occurs prematurely in the magnesium materials tested. The premature linkage is associated with the failure of grain and twin boundaries. Both extension and compression twins have been characterized and contribute to the final failure. The weak correlation between the void fraction and void orientation on failure is a direct consequence of the fact that void linkage is not entirely driven by plasticity. Tomography tests have shown that the failure of the materials is quite complex and 3D techniques must be used to determine where the first failure site occurs.

5. References

- [1] Barnett, M.R., Twinning and the ductility of magnesium alloys: Part I: “Tension” twins. *Materials Science and Engineering: A*, 2007. 464(1–2): p. 1-7.
- [2] Weck, A. and D.S. Wilkinson, Experimental investigation of void coalescence in metallic sheets containing laser drilled holes. *Acta Materialia*, 2008. 56(8): p. 1774-1784.
- [3] Weck, A., et al., Femtosecond laser-based fabrication of a new model material to study fracture. *Applied Physics A*, 2007. 86(1): p. 55-61.
- [4] Puttick, K.E., Ductile fracture in metals. *Philosophical Magazine*, 1959. 4(44): p. 964-969.
- [5] Hosokawa, A., et al., Effect of triaxiality on void growth and coalescence in model materials investigated by X-ray tomography. *Acta Materialia*, 2012. 60(6–7): p. 2829-2839.
- [6] Salvo, L., et al., X-ray micro-tomography an attractive characterisation technique in materials science. *Nuclear Instruments and Methods in Physics Research Section B: Beam Interactions with Materials and Atoms*, 2003. 200(0): p. 273-286.